Possible spin-triplet superconducting phase in the $La_{0.7}Sr_{0.3}MnO_3/YBa_2Cu_3O_7/La_{0.7}Sr_{0.3}MnO_3$ trilayer

K. Dybko,* K. Werner-Malento, P. Aleshkevych, M. Wojcik, M. Sawicki, and P. Przyslupski
Institute of Physics, Polish Academy of Sciences, Al. Lotnikow 32/46, 02-668 Warszawa, Poland
(Received 30 March 2009; revised manuscript received 16 July 2009; published 5 October 2009)

We report on results of conductance spectroscopy measurements in the current-in-plane (CIP) and current-perpendicular-to-plane (CPP) geometries ([001] and [100] directions respectively) of $La_{0.7}Sr_{0.3}MnO_3/YBa_2Cu_3O_7/La_{0.7}Sr_{0.3}MnO_3$ (LSMO/YBCO/LSMO) nonsymmetric trilayer structures in order to search for signature of the formation of spin-triplet phase. This trilayer shows an enhancement of the superconducting transition temperature in magnetic field parallel to the plane. We argue that this enhancement is a result of the formation of spin-triplet phase. The differential conductance (dI/dV) spectra show fully developed zero-bias conductance peaks (ZBCP). The ZBCP measured in CIP geometry demonstrates a sharp shape. This could be attributed to a spin-triplet state arising from the proximity effect at the interface of the half-metal with the *d*-wave superconductor, similar as was predicted theoretically for the *p*-wave superconductor and observed experimentally in *p*-wave Sr_2RuO_4 superconductor. The measurements of the dI/dV in CPP geometry reveal a V shape similar as was experimentally observed in YBCO superconductor and predicted theoretically for superconductor with a $d_{x^2-y^2}$ pairing symmetry of the order parameter.

DOI: 10.1103/PhysRevB.80.144504 PACS number(s): 74.78.Fk, 74.45.+c, 74.25.Fy, 74.25.Nf

I. INTRODUCTION

The competition between antagonistic magnetic and superconducting order parameters in superconducting/ferromagnetic (S/F) systems is responsible for many interesting physical effects. These effects are related with the induced superconducting correlations in the ferromagnet due to the proximity effect, and, contrary, the magnetic moment opposite to that of the F layer, in the diffusive limit, may be induced in the superconducting layer, following the theoretical models of Refs 1 and 2. These features may be revealed through the investigation of the transport and magnetic properties of the S/F interface.

In normal-metal/superconductor (N/S) contacts, the transport properties are governed by local Andreev reflection. In N/high-T_c superconductor contacts, an important role is played by the Andreev bound states (midgap states),[3] which lead to the formation of the zero-bias conductance peak (ZBCP). Theoretical models predict that the response of zero energy states to the proximity of a highly spin polarized system and applied magnetic fields may be a sensitive probe of boundary states at an S/F contact.[4] Systematic studies of *d*-wave superconductor with high spin polarization are particularly interesting as they hold the potential for probing unconventional superconductivity at the S/F interface. Among the theoretical possibilities is that of an induced superconducting condensate in the ferromagnet, which would have an *s*-wave triplet component.[5] For the case where the magnetization of the F region is homogeneous, only the triplet component with projection $S_z=0$ of the total Cooper pair spins is predicted. This is a short-range proximity effect, as, in the diffusive case, the single component penetrates into the *F* region over a short distance of the order $\xi_F=\sqrt{D/h}$, where *D* is the diffusion constant and *h* the exchange field. On the other hand, for a nonhomogeneous magnetization related to the presence of domain walls, a long-range triplet component with $S_z=\pm 1$ may be induced. Then, the authors[6] consider the influence of the relative alignment of the in-plane magnetic moments of the *F* layers in the F/S/F structure. The authors also found that the condensation energy is lowest when magnetic moments in *F* layers are antiparallel.

A long-range proximity effect has been demonstrated experimentally in a $NbTiN/CrO_2/NbTiN$ trilayer structure.[7] These results were explained assuming a conversion from spin singlet- to spin-triplet pairs at the $NbTiN/CrO_2$ interface. Theoretical predictions[8] indeed suggest the possibility of a long-range proximity effect based on the mechanism of quasiparticle spin rotation in the superconductor during reflection events at the half-metal interface. A long-ranged triplet component of the order parameter can be created when spin-flip centers are present in the interface region. It is these spin-triplet pair correlations created *within* the superconductor that then penetrate the ferromagnet.

Recent results[9] of neutron reflectometry measurements on $YPrBaCuO/La_{0.7}Ca_{0.3}MnO_3$ multilayers suggest a possibility of inducing a spin-triplet superconducting phase in manganite layers, which could be the source of long-range proximity effect observed in $La_{0.7}Ca_{0.3}MnO_3/YBa_2Cu_3O_7$ (LCMO/YBCO) multilayers.[10] The aim of this paper is to search for signatures of unconventional superconductivity at the half-metal-singlet *d*-wave superconductor interface in LSMO/YBCO/LSMO trilayer structures and the study of the interface properties. For this, we have investigated subgap transport using conductance spectroscopy and low-field dc magnetoresistance measurements. In order to the study of the subgap transport the key factor are the physical properties of the interface. We have therefore also performed dc magnetization, ferromagnetic resonance (FMR), and nuclear magnetic resonance (NMR) measurements.

II. EXPERIMENTAL

LSMO/YBCO/LSMO trilayer structures were grown by high-pressure sputtering[11] from stoichiometric targets at an

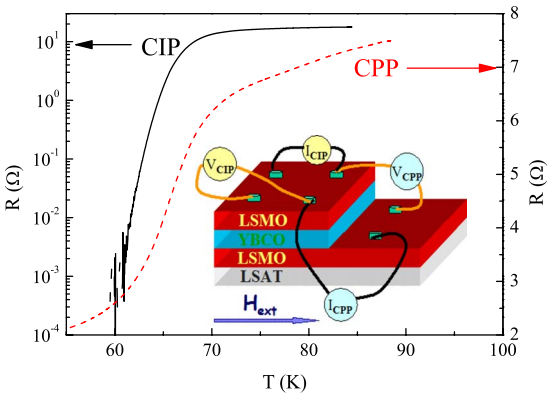

FIG. 1. (Color online) Resistance vs temperature measured in the CIP and quasi-CPP geometry. Inset shows the trilayer geometry used in the experiment.

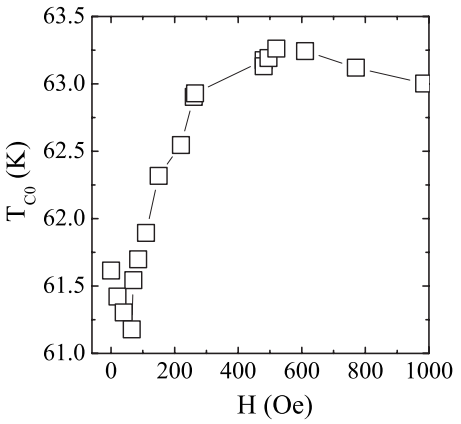

FIG. 2. T_{c0} vs external magnetic field measured in the CIP geometry.

oxygen pressure of 3 mbar and a substrate temperature of 770 °C. High quality epitaxial structure were deposited on [100] oriented $[(LaAlO_3)_{0.3}(Sr_2TaAlO_6)_{0.7}]$ (LSAT) substrates. LSAT has a cubic structure with a lattice constant $a=0.3866$ nm. Bulk $La_{0.7}Sr_{0.3}MnO_3$ (LSMO) is also cubic, with a lattice constant $a=0.387$ nm. There is therefore a good lattice matching between the LSMO and LSAT.[12] After the deposition of the first LSMO layer, the sputtering system was opened and one third of the layer was covered with another substrate. Before the deposition of the consecutive YBCO and LSMO layers, the sample was annealed at deposition temperature in oxygen atmosphere for 30 min. This procedure ensures good surface reconstruction.

The substrate dimensions were 5×10 mm. Transport measurements were performed using the four-point technique in the cryostat equipped with *in situ* rotation gear mechanism. Electrical contacts were deposited on the structures in the form of silver dots, as shown in the inset of Fig. 1. Such a configuration allows measurements in the current-in-plane (CIP, using the four top contacts), as well as the "quasi-current-perpendicular-to-plane" (CPP, with two bottom and two top contacts) geometry.

The dynamical conductance was measured by a standard low-frequency lock-in technique with dc bias or equivalently, by the Delta mode of the Keithley 6221 programmable current source.[13] The resistance and magnetoresistance were measured with a current in the range of $1-10$ μA, unless otherwise stated. The dc magnetization was measured in superconducting quantum interference device in the temperature range of 5–200 K, and magnetic fields of up to 1 kOe. Magnetic properties of the trilayer were also determined using a FMR spectrometer. The FMR measurements were performed in a 5–300 K temperature range using a Bruker EMX X-band (9.25 GHz) electron-spin-resonance spectrometer with a rectangular microwave cavity and a standard phase-sensitive detection technique. The trilayer or single LSMO layer were mounted on a quartz holder, and an external goniometer was used to measure the resonance field as a function of the out-of-plane (θ_H) angle of the external magnetic field (H_{ext}).

^{55}Mn spin-echo NMR experiments were performed at 4.2 K, in zero external magnetic field, and at several values of the rf field excitation in order to optimize the signal intensity at each frequency. NMR spectra were obtained in the frequency range of 250–450 MHz by plotting the optimum spin-echo signal intensity, corrected for the intrinsic enhancement factor and the frequency dependent sensitivity factor,[14,15] at every 1 MHz.

III. RESULTS

A. Conductance spectroscopy and magnetotransport

In Fig. 1 we present the resistance versus temperature $[R(T)]$ curves obtained for the LSMO(16nm)/YBCO(21nm)/LSMO(22nm) nonsymmetric trilayer structure in both the CIP and the CPP geometry. The onset of the superconducting transition is at $T_{c\ onset}\approx70$ K. In the CIP geometry, T_{c0}, defined as the temperature at which the resistance has dropped three orders of magnitude with respect to its normal-state value ($R/R_n=10^{-3}$), is about 61 K. The $R(T)$ curve measured in the quasi-CPP geometry shows some residual resistance even at $T\sim50$ K. This is due to the fact that in this geometry, apart from the resistance of the YBCO layer in the c-axis direction, one measures the additional resistance of the bottom LSMO layer (see Fig. 1).

In the next step, we have measured the resistive transition in a magnetic field oriented parallel to the sample,[16] see Fig. 2. It is seen that lowest superconducting transition temperature T_{c0} is obtained for a field of about 65 Oe, which corresponds to the coercivity field of the LSMO. A further increase of the magnetic field induces an increase of T_{c0} of about 1.6 K as compared to the demagnetized state ($H=O$). The maximum enhancement is obtained in a magnetic field of about 500 Oe. Above this field we observe a monotonic decrease of T_{c0}.

The anomalous behavior of the T_{c0} vs magnetic field curve is attributable to the influence of several mechanisms including the stray field of magnetic domain walls, the spin polarization of the current, or the formation of a spin-triplet superconducting state.[16] Magnetotransport measurements on LCMO/YBCO/LCMO trilayers[17] suggest that the enhancement of the superconducting state is governed by the inverse superconducting spin switch effect. This mechanism has that

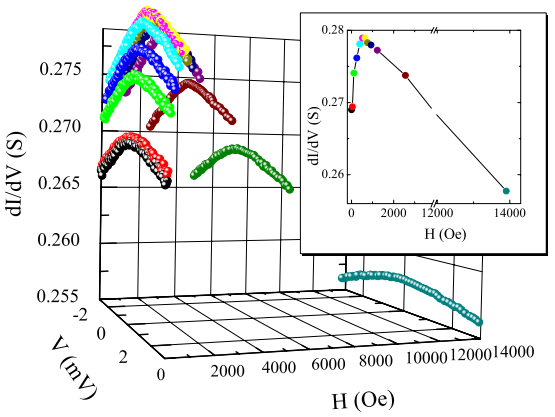

FIG. 3. (Color online) Dynamical conductance, dI/dV, vs V and magnetic field measured at $T=64.4$ K in CPP geometry. Inset: maximum dI/dV vs H.

for parallel alignment of the magnetic moments of the LCMO layers, the electrons transmitted from one electrode can enter the other LCMO electrode, while for an antiparallel alignment the electrons will be *reflected* from the second LCMO electrode. In this way, the superconducting transition temperature of the trilayer structure is reduced.

Tunneling spectroscopy provides important information on the superconducting pairing symmetry of the order parameter and the spin-dependent subgap transport in the LSMO/YBCO/LSMO trilayers. We have measured the dynamical conductance, dI/dV vs V, in both the CIP and CPP geometries ([100] and [001] directions). The spectra show well-developed ZBCP structures, such as commonly observed in $YBa_2Cu_3O_7$, where they were explained as arising from low energy Andreev bound states due to the predominantly d-wave symmetry of the superconducting order parameter. In the present LSMO/YBCO/LSMO trilayers, we observe a broad "V" shape of the ZBCP peak in the CPP geometry (as shown in Fig. 3) and a sharp peak in the CIP geometry (see Fig. 4).

Two features of the ZBCP are intriguing. First, the spectral evolution of the ZBCP versus magnetic field shows a non–monotonic behavior of the maximum of the dynamical conductivity dI/dV, which has a peak at a magnetic field of

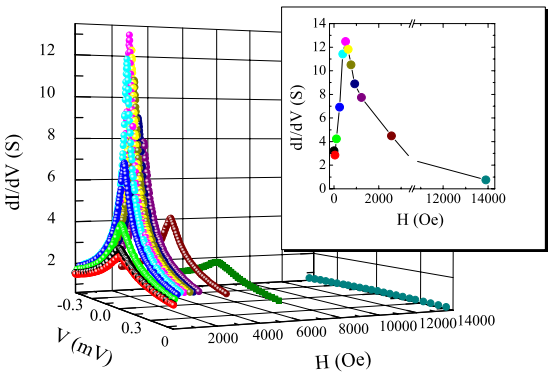

FIG. 4. (Color online) Dynamical conductance, dI/dV, vs V and magnetic field measured at $T=64.4$ K in the CIP geometry. Inset: maximum dI/dV vs H.

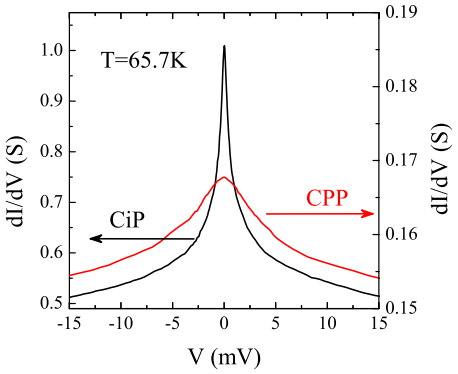

FIG. 5. (Color online) Dynamical conductance vs bias voltage V measured at zero magnetic field in the CIP and CPP geometries, for the LSMO(22 nm)/YBCO(21 nm)/LSMO(16 nm) trilayer.

about 500 Oe for both the CIP and CPP geometries. A theoretical model for a d-wave superconductor /multidomain ferromagnet bilayer, predicts an enhancement of the proximity effect.[18] However, the presence of domain walls generates an odd-frequency triplet s-wave component of the superconducting condensate. Second, the ZBCP structures do not demonstrate any form of splitting in a magnetic field. A very strong enhancement of dI/dV vs H is observed for the CIP geometry, the maximum conductivity in magnetic field is growing with a factor of up to 4 when compared to the measurement in zero magnetic field. Much lower enhancement (factor 1.04) of the dynamical conductance was observed in CPP geometry (inset in Fig. 3). The dI/dV peak disappears above $T_{c\ onset}$ for CIP and CPP geometries.

According to experimental[3,19–22] and theoretical[23] results on dirty unconventional contacts, a "V"-shaped ZBCP would correspond to a d-wave symmetry of the order parameter, whereas a sharp ZBCP corresponds to a superconducting state with p-wave symmetry of the order parameter. "V"-shaped structures have been observed in several trilayer structures in the CPP geometry (see Figs. 5 and 6. For instance, the results presented in Fig. 6 were obtained for a LSMO(10nm)/YBCO(21nm)/LSMO(22nm) trilayer with a $T_{c\ onset}$ of approximately 72 K.[24] In contrast, in CIP geometry the dynamical conductivity always presents a sharp structure. The different shape of the ZBCP in CPP and CIP

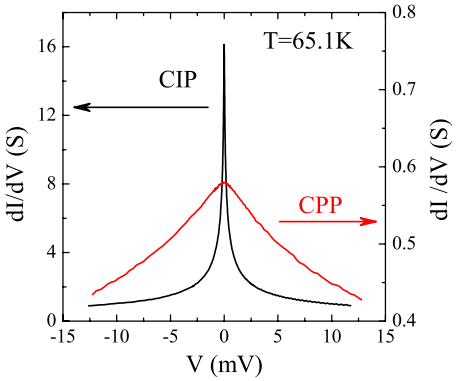

FIG. 6. (Color online) Dynamical conductance vs bias voltage V measured at zero magnetic field in the CIP and CPP geometries for the LSMO(22 nm)/YBCO(21 nm)/LSMO(10 nm) trilayer.

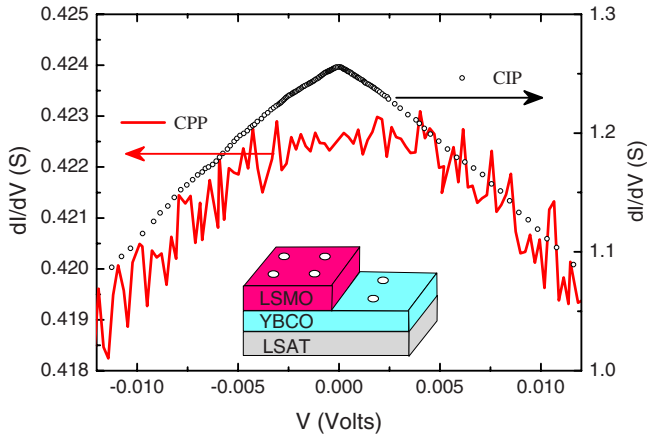

FIG. 7. (Color online) Dynamical conductance vs bias voltage V measured at zero magnetic field in the CIP and CPP geometries recorded at $T=86$ K for the bilayer LSMO(50 nm)/YBCO(60 nm) ($T_c=88$ K).

geometry could be a consequence of the presence of *different* superconducting states, i.e., a state with d-wave symmetry of the order parameter in the bulk of the $YBa_2Cu_3O_7$ layer, and an induced state with p-wave symmetry of the order parameter at the LSMO/YBCO interfaces. In the CIP geometry in low fields, one probes a large area of nonuniform magnetization because of the noncollinear alignment of the magnetic moments in the LSMO layers and because of the presence of domain walls. The presence of a nonuniform magnetization leads to the presence of zero-bias states and possibly the spin-triplet state.

The theoretical model[25] treating the contact between a normal metal and a ferromagnetic superconductor predicts the appearance of ZBCP in the tunnelling spectra for spin-triplet equal pairing order parameter. Similar to our differential conductance results measured in CIP geometry, the tunnelling spectroscopy obtained on Sr_2RuO_4 system[26] also demonstrates the existence of sharp ZBCP structures. These were interpreted as a signature of the p-wave symmetry of the order parameter in that compound.

In Fig. 7 we present the dynamical conductance measurements for the LSMO(50nm)/YBCO(60nm) bilayer. The bilayer structure was fabricated in similar way as the trilayer structures. Those samples have steplike structure and were made with the opening of the sputtering system after deposition of the bottom layer. The results of dI/dV measurements for both CIP and CPP geometries indicate a V-like shape. It is significantly different than the results obtained for the trilayer structures. This result implies that rather the noncollinear alignment of magnetic moments in LSMO layers is responsible for the occurrence of the sharp peak in CIP geometry of the trilayers. The magnetic inhomogeneity resulted from the domain structure (domain walls) does not produce the triplet phase for the bilayer structure. The fabrication procedure of the step like structure does not have any influence on the experimental results. In Fig. 8 the dynamical conductance measurements for the LSMO(8 nm)/YBCO(9.6 nm)/LSMO(8 nm) trilayer deposited in single process are presented. It is seen that qualitatively the shape of the ZBCP measured in CIP geometry does not depend on the fabrication process.

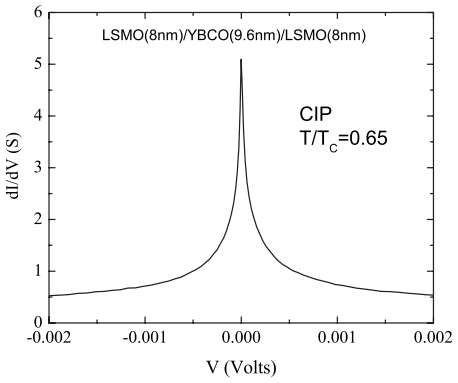

FIG. 8. Dynamical conductance vs bias voltage V measured at zero magnetic field in the reduced temperature $t=T/T_c=0.65$ in the CIP geometry for the LSMO(8 nm)/YBCO(9.6 nm)/LSMO(8 nm) trilayer.

The magnetoresistance was measured as function of the magnetic field strength by varying the in-plane magnetic field in the range from −1.5 kOe to 1.5 kOe. During the measurements, the temperature stabilization was controlled with an accuracy better than 10 mK. Figure 9 shows representative low-field magnetoresistance curves measured above and below $T_{c\ onset}$. Above $T_{c\ onset}$, the magnetoresistance was defined as $MR \equiv (R-R_{H=1000\ Oe})/R_{H=1000\ Oe}$. Below $T_{c\ onset}$ the magnetoresistance was defined as $MR \equiv (R$

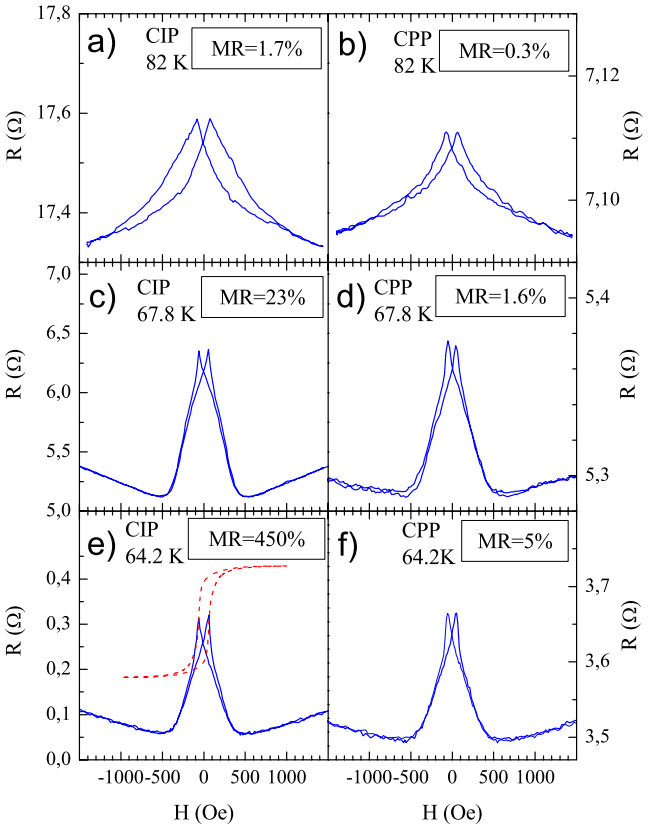

FIG. 9. (Color online) Resistance vs H measured in CIP (left panel) and CPP(right panel) above and below superconducting transition $T_{c\ onset}$ ($I=10$ μA, $H \| I$). For clarity, in panel (e) the $M(H)$ hysteresis loop is superimposed on $R(H)$ curve.

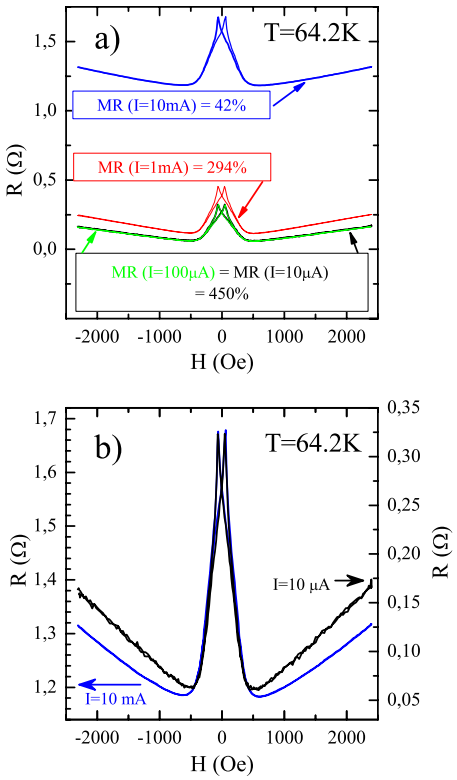

FIG. 10. (Color online) (a) MR vs H for different measurement currents: 10, 100 μA, 1, and 10 mA; (b) the position of minimum of the magnetoresistance and the background shape dependence on applied current for $I=10$ μA and $I=10$ mA.

$-R_{\min})/R_{\min}$. Figures 9(a) and 9(b) show that in CIP and CPP geometries, MR($T=82$ K) is 1.7% and 0.3%, respectively. In contrast, below $T_{c\ onset}$, at $T=67.8$ K, MR in the CIP and CPP geometries has a value 23% and 1.6% as shown in Figs. 9(c) and 9(d). Therefore, decreasing temperature below $T_{c\ onset}$ significantly enhances MR. A further decrease in the temperature increases the value of MR even further: MR(64.2 K)=440% in the CIP geometry, and 5% in the CPP geometry.

Figure 9(e) also shows the hysteresis loop of the magnetization of the LSMO layers. The magnetoresistance clearly exhibits two well-resolved peaks with a hysteretic character. The maximum of the magnetoresistance occurs at the coercive field H_c. Such features were previously observed in single LSMO layers, where their origin was attributed to spin-dependent scattering at grain boundaries and/or magnetic domain walls.[27] The minimum of MR in Fig. 9 occurs for a magnetic field of approximately 500 Oe, i.e., lower than the saturation field of the trilayer and even othan that of the bottom LSMO layer. At higher fields the magnetoresistance becomes positive. The shape of the magnetoresistance curves measured in the CIP and CPP geometries at high fields are similar, which indicates that at high fields, the mechanism responsible for the ZBCP is similar in the two cases.

Given the peaked nature of the ZBCP, the magnetoresistance also strongly depends on the value of the measuring current [see Fig. 10(a)]. The position of the magnetoresistance minimum also depends on the value of the measuring current, as shown in Fig. 10(b). Up to a value $I=100$ μA,

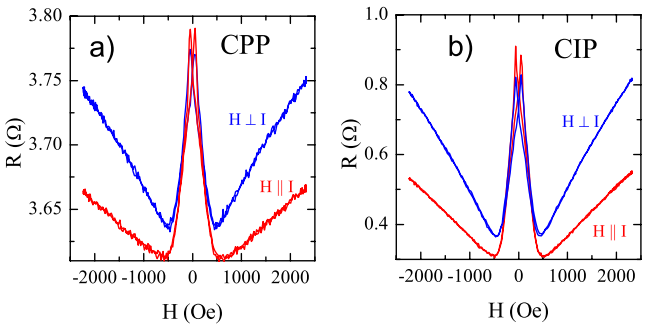

FIG. 11. (Color online) Comparison of MR in the CPP (a) and CIP (b) configurations for H parallel and perpendicular to I measured at $T=65$ K.

the position of the minimum does not change; a current of 10 mA shifts the minimum by about 120 Oe in comparison to the minimum position for $I<100$ μA. At magnetic fields higher than 500 Oe, a large measurement current also changes the shape of the magnetoresistance background from linear to parabolic. Similarly, the MR background change is visible in Figs. 11(a) and 11(b) for both CPP and CIP geometries, when rotating the sample from $H\|I$ to $H\perp I$ configuration. A slight change of the MR peak size can also be noticed, as opposed to analogous situation in LCMO/YBCO/LCMO systems.[28]

In the LCMO/YBCO/LCMO trilayers of Ref. 28 and 29, three mechanisms were proposed as being at the origin of the magnetoresistive behavior. These are dissipation due to vortex motion, the anisotropy of the magnetoresistance in manganites, and spin-dependent transport. The authors conclude that the most probable mechanism responsible for the magnetoresistance effect is spin-dependent transport. On the other hand, the authors of Ref. 30 claim that in LSMO/YBCO/LSMO trilayers, the resistance switching effect is caused by magnetic stray–field from the ferromagnetic layers. The authors suggest also that the interface roughness plays an important role in this effect.

B. Magnetic characterization

In order to understand the anomalous transport properties, we have measured the magnetic properties of the trilayer structure in the vicinity of the superconducting transition. The $M(H)$ curve (Fig. 12) shows that magnetic saturation of the magnetic moment of the trilayer is reached at about 750 Oe. The coercive field of the trilayer is approximately 66 Oe. The inset in Fig. 12 shows an enlargement of the $M(H)$ curve, demonstrating a clear plateau of $M\approx 0$. In a next step, we have measured the magnetic properties of the bottom LSMO layer. It is seen that the magnetic moment saturates at about 600 Oe and that the coercive field is approximately 49 Oe. The bottom LSMO layer is therefore magnetically softer than the top LSMO layer. It is also seen that the magnetic moment per unit volume of the bottom layer is larger than the magnetic moment of the whole trilayer structure. Our earlier experiment[31] performed on LSMO/YBCO superlattices showed that due to hole charge transfer from YBCO to LSMO layers at least three unit cells of the LSMO layer

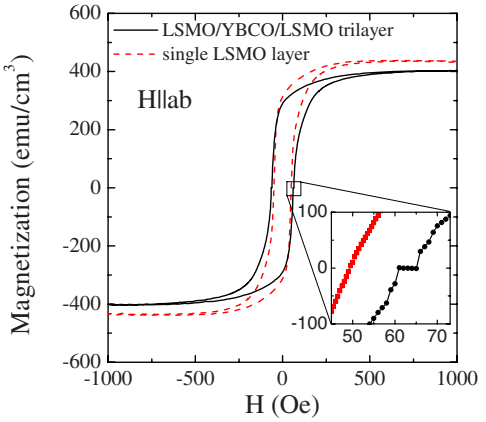

FIG. 12. (Color online) Hysteresis loops $M(H)$ of the trilayer and the bottom LSMO layer, measured at $T=64$ K (low-field region expanded).

show a zero net magnetic moment. The observation of the induced unidirectional magnetic anisotropy (exchange bias) indicated that this part of LSMO layer shows antiferromagnetic (AF) order. This is due to the decrease in the ratio of Mn^{+3}/Mn^{+4} ions, although the nominal composition $La_{1-x}Sr_xMnO_3$ is at the doping level $x=0.3$. On the other hand, the onset of the superconducting transition was observed for LSMO/YBCO superlattices[31] with YBCO thickness equal and larger than two c-axis unit cells. This observation indicates that at the interface between LSMO and YBCO layers a single, YBCO layer of thickness equal to the c-axis lattice parameter is nonsuperconducting. Later neutron polarization studies[32] have fully confirmed this finding. The appearance of antiferromagnetic coupling in an LCMO layer near to the LCMO/YBCO interface is also predicted theoretically.[33] On the other hand, x-ray circular dichroism studies of LCMO/YBCO multilayers[34] indicate the polarization of Cu ions close to the LCMO surface.

To gain information on the contribution to magnetic moment of each LSMO layer in the trilayer structure we have performed FMR spectroscopy characterization of the trilayer structure and single bottom LSMO layer. Figure 13 shows the FMR spectra recorded for the trilayer and the single LSMO layer in (a) perpendicular and (b) parallel orientation

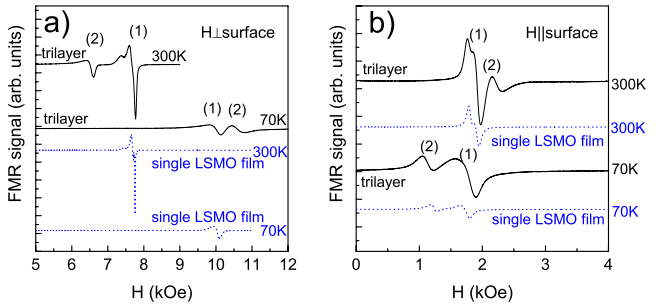

FIG. 13. (Color online) The comparison of the FMR spectra of the trilayer and single LSMO bottom layer, recorded with the external magnetic field oriented perpendicular (a) and parallel (b) to the film plane, at 70 and 300 K; labels (1) and (2) denote two main resonance lines in the trilayer—description in text.

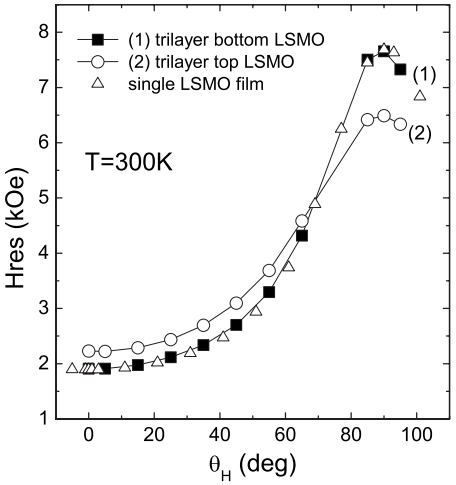

FIG. 14. The angular dependence of the resonance peaks positions of the trilayer and single LSMO layer at room temperature.

of external magnetic field. It is seen that the trilayer spectra exhibit the two resonance lines. The spectrum measured in perpendicular magnetic field of single LSMO layer shows one FMR peak, whereas the spectrum recorded in magnetic field parallel to the film surface [Fig. 13(b)] at $T=70$ K shows two resonance peaks. The appearance of the second resonance peak for single LSMO layer could result form the phase separation observed for strained epitaxial films. Such an effect was observed in LCMO thin films deposited on $SrTiO_3$ substrates[15] and in LSMO films.[35] This means that in order to produce ferromagnetism in manganite layers their thickness should be above certain critical thickness. The authors suggest that close to the substrate three different phases are formed such as nonferomagnetic insulating, ferromagnetic insulating and ferromagnetic metallic. In our case the appearance of the second peak for single layer could result form ferromagnetic insulating phase. The spectrum recorded for the trilayer for both orientations and for all measured temperatures shows two resonance lines. As it is seen in Fig. 13 the position of more intensive resonance peak labeled as (1) coincides with the position of the FMR peak of the single LSMO film, moreover their angular variation at room temperature is the same (Fig. 14). Therefore it is reasonably to assume that peak (1) corresponds to the bottom LSMO layer of the trilayer structure, and consequently, peak (2) as originated from the top LSMO layer.

The integrated intensity of the resonance lines is proportional to the number of magnetic ions in each LSMO layer, this enables the additional identification each LSMO layer in the trilayer structure. The calculated ratio of the integrated intensity of lines (1) and (2) I_1/I_2 varies between 1.3 and 1.6 for different orientations. This ratio is close to the expected value $22(\text{nm})/16(\text{nm})=1.375$, which again confirms that the line (1) corresponds to the bottom LSMO layer, whereas the line (2) corresponds the top LSMO layer.

Figures 15(a) and 15(b) show the FMR spectra recorded in the temperature range of 300–50 K for perpendicular and parallel external magnetic field. It is seen that as the temperature decreases, the position of line (2) shifts stronger than the line (1), which indicates that the magnetic moment or the

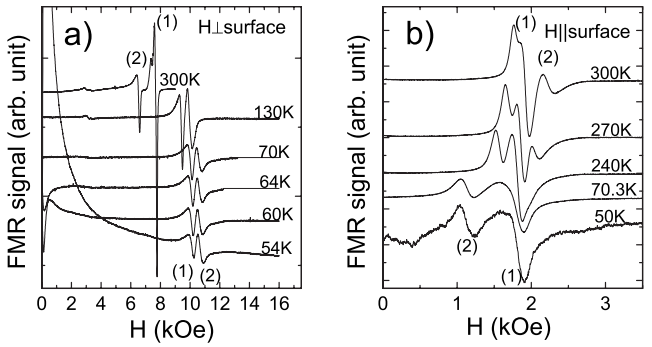

FIG. 15. The FMR spectra of the trilayer recorded for (a) perpendicular and (b) parallel orientations of the external magnetic field in temperature range of 50K–300K.

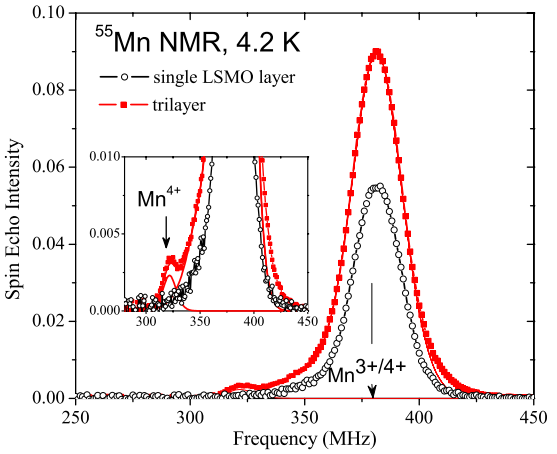

FIG. 16. (Color online) ^{55}Mn NMR spectra recorded for LSMO(22 nm)/YBCO(21 nm)/LSMO(16 nm) trilayer (full squares) and single LSMO(22 nm) film (empty circles). Inset: the same spectra showing the details of NMR intensity at about 320 MHz.

anisotropy of the upper LSMO layer changes strongly than the anisotropy of the bottom LSMO layer. It is also seen that at room temperature, both LSMO layers are ferromagnetically ordered with a spontaneous in-plane magnetic moment. The resonance lines have different positions due to the difference of the spontaneous magnetization and the magnetic anisotropy of the bottom and top LSMO layers. Both lines [especially line (1)] are asymmetrical, with a nonregular shape, indicating that the magnetic moments are distributed nonuniformly along the normal to the trilayer surface.

In the temperature range of 50–70 K the resonance lines do not change their position [Figs. 15(a) and 15(b)]. In this temperature range the intensity of line (1) decreases in contrary to the increase of the intensity of the line (2). From the fact that the lines do not change their position, it is reasonable to assume that the spontaneous magnetization and anisotropy remain constant. Therefore, the changes of the lines' intensities could result from the change of the number and the shape of the domain-wall configuration. Below 60 K, strong nonresonant absorption of the microwaves at zero magnetic field appears due to the superconductivity of the YBCO layer.

In order to get information about the origin of the changes of the magnetic properties of the LSMO thin films in the vicinity of the LSMO/YBCO interface in the LSMO/YBCO/LSMO trilayer structure, a ^{55}Mn NMR experiment has been carried out on the LSMO/YBCO/LSMO trilayer as well as on the bottom single LSMO layer. NMR applied to the study of mixed-valence manganese perovskites can help to discriminate between different valence states of the Mn ions, and can also distinguish between a possible localized versus a delocalized nature of the charge carriers in the LSMO system.

Such information is obtained from the frequency f_{res} of the ^{55}Mn resonance line, which is in turn determined by the corresponding value of the local field B_{Mn} experienced by the ^{55}Mn nuclei: $f_{res}=\gamma B_{\mathrm{Mn}}$, where $\gamma/2\pi=10.553$ MHz T^{-1}. B_{Mn} arises mainly from the hyperfine interaction, which depends on the local Mn moment S. It is well documented in literature that in bulk samples of LSMO perovskites, localized Mn^{4+} moments with spin $S=3/2$ (due to $3t_{2g}$ core electrons) have a resonance frequency in the range of 310–330 MHz.[36] The electrons localized in $3e_g$ states with $S=2$ shift the NMR frequency of localized Mn^{3+} ions to the 400–430 MHz range. The signal corresponding to the double exchange state of the Mn ions in the ferromagnetic metallic phase of the manganite with fast hopping of electrons between the Mn^{3+} and Mn^{4+} sites is characterized by a single line centered at an intermediate frequency, which is determined by the exact Mn^{3+}/Mn^{4+} ratio. In the case of optimally doped $La_{0.7}Sr_{0.3}MnO_4$ compound this frequency is approximately 380 MHz.[36]

Figure 16 shows the ^{55}Mn NMR spectra of the LSMO/YBCO/LSMO trilayer and of the LSMO single layer. The NMR intensity has been normalized to the film surface, so that the intensity of the spectra corresponds to the effective LSMO layer thickness of each layer. The dominating line in both spectra corresponds to the mixed-valence Mn^{+3}/Mn^{+4} state with $f_{res}\gamma\times 380$ MHz (Ref. 36) as expected for the double exchange–mediated metallic state. Inspection of the spectrum recorded for the trilayer reveals that, in addition to this peak, there is another broad peak at a lower frequency (315 MHz), with lower intensity. This secondary peak is attributed to the existence of localized ferromagnetic Mn^{4+} states. The absence of the second peak in the spectrum of single LSMO layer indicates that there are no localized states of Mn ions.

IV. DISCUSSION

The physics of subgap transport due to a quasiparticle current from the ferromagnet through a superconductor in a F/S/F structure is a complex problem. In LSMO/YBCO/LSMO trilayer, we have observed an enhancement of the critical temperature T_{c0} in parallel magnetic field at about 500 Oe. The maximum of the enhancement occurs at a magnetic field that is lower than the saturation field of the trilayer or the saturation field of the bottom LSMO layer. As mentioned above, several mechanisms could be responsible for such behavior. These are the stray fields from the magnetic domain walls, the spin polarization of the current, or the formation of an odd triplet superconducting state at the interface between the LSMO and the YBCO.

An odd-parity, triplet superconducting state could result from a nonhomogeneous magnetization or from a non–collinear alignment of the magnetic moments in the LSMO layers at the optimal magnetic field, or from stray fields of the domain walls. Our conductance spectroscopy measurements reveal the existence of a ZBCP resulting from Andreev bound states at the YBCO/LSMO interface. The existence of the midgap states in F/S structures was also observed in several other experiments[37–39] In our experiment, the shape of the ZBCP in the CIP geometry was sharp, similar to observed in the Sr_2RuO_4 compound[26] with spin-triplet *p*-wave symmetry and predicted theoretically for the superconductor with *p*-wave symmetry.

Recent results[9] of neutron reflectometry measurements on a YPrBaCuO/LCMO multilayers indicate a giant superconductivity modulation of the ferromagnetic magnetization. Based on the experimental results the authors suggest a possibility of inducing a spin-triplet superconducting phase in manganite layers.

In the CPP geometry a "V"-shaped ZBCP-like structure was recorded which is similar to that observed for YBCO system with *d*-wave symmetry[40] and predicted theoretically.[41,42] The theoretical model of F/d-wave superconductor/F structures developed in Ref. 43 predicts the appearance of a spin-triplet states in such systems. According to the model, a nonlocal Andreev reflection can be induced due to a noncollinear magnetization. Then, the incident electron and the Andreev reflected hole come from the same spin subband, forming a triplet pair with parallel spins, while in the usual Andreev process they come from different subbands leading to spin singlet pairing with opposite spins. The model predicts that for highly polarized F layers the ZBCP splits, and is transformed into a zero-bias conductance dip (ZBCD). The ZBCP splitting is attributed to broken time-reversal symmetry states. The authors suggest that the conductance within the *d*-wave gap along the 110 direction exhibits ZBCD in the parallel alignment ($\alpha=0$) of the magnetic moments due to the absence of usual Andreev reflection. The change from $\alpha=0$ to $\alpha=\pi/2$ should convert the ZBCD to ZBCP.

In the case of LSMO/YBCO/LSMO no splitting of the ZBCP was observed. However, as was presented above through FMR and NMR spectroscopy, the interface between the LSMO and YBCO layer is very complex. Due to the hole transfer from YBCO, part (three unit cells) of the LSMO layer is converted into an AF state. Therefore, instead of a nominal F/S interface we have an effective F/AF/I/S interface since a YBCO layer of thickness of at least one unit cell is not superconducting but insulating. We cannot exclude the phase separation in the top LSMO layer. In $[\mathrm{LSMO}(8\ \mathrm{u.c.})/\mathrm{YBCO}(1\ \mathrm{u.c.})]\times 16$ superlattice[44] we have observed semiconducting like behavior of resistance as a function temperature. Such behavior indicates that at latest one-unit-cell-thick YBCO layer in heterostrcture is insulating. The existence of the insulating native barrier[45] at the LSMO/YBCO interface was also suggested in LSMO/YBCO junction. Therefore, this could be the reason that we do not observe the splitting of the ZBCP, in contrary to the observation reported on $SrRuO_3$/YBCO bilayer.[39] On the other hand, we observe a nonmonotonic dependence of the ZBCP vs external magnetic field.

The observation of the occurrence of the maximum T_{c0} at about 500 Oe could result from optimal domain configuration (noncollinearity) for the formation of the spin-triplet phase. If the spin-triplet state is formed, than it has the maximum of the free energy at this field. This observation could alternatively result from an optimal configuration of the domain walls in LSMO layers, which partially lifts the exchange field of the LSMO ferromagnet and in consequence induce the increase of the T_{c0}. The appearance of the triplet phase penetrating the LSMO can enhance the conductivity.

V. CONCLUSIONS

In conclusion, we find that an enhancement of T_{c0} in LSMO/YBCO/LSMO occurs in parallel magnetic field of about 500 Oe i.e., below the saturation of the magnetization of the trilayer and the bottom LSMO layer. We have argued that the formation of the spin-triplet superconducting phase is responsible for this enhancement. In the trilayer this magnetic field can produce the optimal magnetic inhomogeneity, which leads to the formation of spin-triplet superconducting phase. The measurements in CIP geometry of differential conductivity demonstrate a sharp ZBCP in qualitative agreement with the theoretical model. Such feature was observed experimentally in Sr_2RuO_4 *p*-wave superconductor. The measurements of differential conductivity in CPP geometry demonstrate "V" shape peak similar as was observed for the YBCO *d*-wave superconductor. This is due to the fact that much smaller area of the trilayer is probed, therefore the magnetization inhomogeneity has smaller influence on the differential conductivity. Both ZBCP anomalies show nonmonotonic dependence of dI/dV vs the magnetic field.

A significant increase of differential conductivity is observed for the same value of magnetic field at which the T_{c0} enhancement is observed. The weak dependence of dI/dV vs H above the maximum dI/dV vs H shows a robust behavior, which could be a result of the formation of spin-triplet phase. Magnetoresistance measurements demonstrate also the occurrence of the minimum at the same magnetic field where the dI/dV reaches the maximum. Such feature could be the result of the maximum of the free condensation energy of the spin-triplet superconducting phase. However, no splitting of ZBCP was observed in magnetic field. It is attributed to the complex interface region, namely F/AF/I/S, which is due to hole charge transfer from YBCO to LSMO layers.

Note added in proof. Recently, we became aware of the article by Hu *et al.*[46] which confirms our finding about the occurrence of the spin-triplet superconducting phase in manganite/cuprate heterostructures by the use of the angular magnetoresistance measurements.

ACKNOWLEDGMENT

This work was supported by the Ministry of Sciences and Higher Education under Research Project No. MNiSW-1 P03B 122 30 for the years 2006–2009.

*krzysztof.dybko@ifpan.edu.pl

[1] F. S. Bergeret, A. F. Volkov, and K. B. Efetov, Phys. Rev. B **69**, 174504 (2004).
[2] F. S. Bergeret, A. F. Volkov, and K. B. Efetov, Europhys. Lett. **66**, 111 (2004).
[3] Y. Dagan, A. Kohen, G. Deutscher, and A. Revcolevschi, Phys. Rev. B **61**, 7012 (2000).
[4] S. Kashiwaya, Y. Tanaka, N. Yoshida, and M. R. Beasley, Phys. Rev. B **60**, 3572 (1999).
[5] F. S. Bergeret, A. F. Volkov, and K. B. Efetov, Phys. Rev. Lett. **86**, 4096 (2001).
[6] K. Halterman, P. H. Barsic, and O. T. Valls, Phys. Rev. Lett. **99**, 127002 (2007).
[7] R. S. Keizer, S. T. B. Goennenwein, T. M. Klapwijk, G. Miao, G. Xiao, and A. Gupta, Nature (London) **439**, 825 (2006).
[8] M. Eschrig, J. Kopu, J. C. Cuevas, and G. Schon, Phys. Rev. Lett. **90**, 137003 (2003).
[9] J. Hoppler, J. Sthan, Ch. Nidermayer, V. K. Malik, H. Boyanfif, A. J. Drew, M. Rossle, A. Buzdin, G. Cristiani, H. U. Habermeier, B. Keimer, and C. Bernhard, Nature Mater. **8**, 315 (2009).
[10] V. Pena, Z. Sefrioui, D. Arias, C. Leon, J. Santamaria, M. Varela, S. J. Pennycook, and J. L. Martinez, Phys. Rev. B **69**, 224502 (2004); Z. Sefrioui, D. Arias, V. Pena, J. E. Villegas, M. Varela, P. Prieto, C. Leon, J. L. Martinez, and J. Santamaria, *ibid.* **67**, 214511 (2003).
[11] P. Przyslupski, A. Wisniewski, R. Szymczak, and J. Igalson, Czech. J. Phys. **46**, 1355 (1996); P. Przyslupski, S. Kolesnik, E. Dynowska, T. Skoskiewicz, and M. Sawicki, IEEE Trans. Appl. Supercond. **7**, 2192 (1997); P. Przyslupski, Acta Phys. Pol. **92**, 127 (1997).
[12] P. Przyslupski, Phys. Status Solidi C **2**, 1625 (2005).
[13] A. Daire, *An Improved Method for Differential Conductance Measurements*, (Keithley White Paper, Cleveland, OH, 2005).
[14] P. Panissod, M. Malinowska, E. Jedryka, M. Wojcik, S. Nadolski, M. Knobel, and J. E. Schmidt, Phys. Rev. B **63**, 014408 (2000).
[15] M. Bibes, L. Balcells, S. Valencia, J. Fontcuberta, M. Wojcik, E. Jedryka, and S. Nadolski, Phys. Rev. Lett. **87**, 067210 (2001).
[16] K. Dybko, K. Werner Malento, M. Sawicki, and P. Przyslupski, EPL **85**, 57010 (2009).
[17] N. M. Nemes, M. Garcia-Hernandez, S. G. E. teVelthuis, A. Hoffmann, C. Visani, J. Garcia-Barriocanal, V. Pena, D. Arias, Z. Sefrioui, C. Leon, and J. Santamaria, Phys. Rev. B **78**, 094515 (2008).
[18] A. F. Volkov and K. B. Efetov, Phys. Rev. Lett. **102**, 077002 (2009).
[19] J. Y. T. Wei, N. C. Yeh, D. F. Garrigus, and M. Strasik, Phys. Rev. Lett. **81**, 2542 (1998).
[20] G. Koren and N. Levy, Europhys. Lett. **59**, 121 (2002).
[21] W. Wang, M. Yamazaki, K. Lee, and I. Iguchi, Phys. Rev. B **60**, 4272 (1999).
[22] S. Kashiwaya and Y. Tanaka, Rep. Prog. Phys. **63**, 1641 (2000).
[23] Y. Tanaka and S. Kashiwaya, Phys. Rev. B **70**, 012507 (2004).
[24] P. Przyslupski, K. Dybko, A. Tsarou, K. Werner Malento, M. Sawicki, F. Laviano, L. Gozzellino, and E. Mezzetti, Acta Phys. Pol. **114**, 15 (2008).
[25] T. Yokoyama, Y. Tanaka, and A. A. Golubov, Phys. Rev. B **75**, 134510 (2007).
[26] Z. Q. Mao, K. D. Nelson, R. Jin, Y. Liu, and Y. Maeno, Phys. Rev. Lett. **87**, 037003 (2001).
[27] J. Wolfman, A. M. Haghiri-Gosnet, B. Raveau, C. Vieu, E. Cambril, A. Cornette, and H. Launois, J. Appl. Phys. **89**, 6955 (2001); S. Y. Yang, W. L. Kuang, Y. Liou, W. S. Tse, S. F. Lee, and Y. D. Yao, J. Magn. Magn. Mater. **268**, 326 (2004).
[28] C. Visani, V. Pena, J. Garcia-Barriocanal, D. Arias, Z. Sefrioui, C. Leon, J. Santamaria, N. M. Nemes, M. Garcia-Hernandez, J. L. Martinez, S. G. E. teVelthuis, and A. Hoffmann, Phys. Rev. B **75**, 054501 (2007).
[29] V. Pena, Z. Sefrioui, D. Arias, C. Leon, J. Santamaria, J. L. Martinez, S. G. E. teVelthuis, and A. Hoffmann, Phys. Rev. Lett. **94**, 057002 (2005).
[30] M. van Zalk, M. Veldhorst, A. Brinkman, J. Aarts, and H. Hilgenkamp, Phys. Rev. B **79**, 134509 (2009).
[31] P. Przyslupski, I. Komissarov, W. Paszkowicz, P. Dluzewski, R. Minikayev, and M. Sawicki, Phys. Rev. B **69**, 134428 (2004).
[32] A. Hoffmann, S. G. E. teVelthuis, Z. Sefrioui, J. Santamaria, M. R. Fitzsimmons, S. Park, and M. Varela, Phys. Rev. B **72**, 140407(R) (2005).
[33] W. Luo, S. J. Pennycook, and S. T. Pantelides, Phys. Rev. Lett. **101**, 247204 (2008).
[34] J. Chakhalian, J. W. Freeland, G. Srajer, J. Strempfer, G. Khaliullin, C. Cezar, T. Charlton, R. Dalgliesh, C. Bernhard, G. Cristani, H. U. Habermier, and B. Keimer, Nat. Phys. **2**, 244 (2006).
[35] M. Huijben, L. W. Martin, Y. H. Chu, M. B. Holcomb, P. Yu, G. Rijnders, D. H. A. Blank, and R. Ramesh, Phys. Rev. B **78**, 094413 (2008).
[36] G. Matsumoto, J. Phys. Soc. Jpn. **29**, 606 (1970).
[37] Z. Y. Chen, A. Biswas, I. Zutic, T. Wu, S. B. Ogale, R. L. Greene, and T. Venkatesan, Phys. Rev. B **63**, 212508 (2001).
[38] P. S. Luo, H. Wu, F. C. Zhang, C. Cai, X. Y. Qi, X. L. Dong, W. Liu, X. F. Duan, B. Xu, L. X. Cao, X. G. Qiu, and B. R. Zhao, Phys. Rev. B **71**, 094502 (2005).
[39] I. Asulin, O. Yuli, I. Felner, G. Koren, and O. Millo, Phys. Rev. B **76**, 064507 (2007).
[40] R. Beck, Y. Dagan, A. Milner, A. Gerber, and G. Deutscher, Phys. Rev. B **69**, 144506 (2004).
[41] Y. Tanaka and S. Kashiwaya, Phys. Rev. Lett. **74**, 3451 (1995).
[42] S. Kashiwaya, Y. Tanaka, M. Koyanagi, and K. Kajimura, Phys. Rev. B **53**, 2667 (1996).
[43] Z. Ping Niu and D. Y. Xing, Phys. Rev. Lett. **98**, 057005 (2007).
[44] P. Przyslupski, I. Komissarov, W. Paszkowicz, P. Dluzewski, R. Minikayev, and M. Sawicki, J. Appl. Phys. **95**, 2906 (2004).
[45] A. Sawa, S. Kashiwaya, H. Obara, H. Yamasaki, M. Koyanagi, N. Yosida, and Y. Tanaka, Physica C **339**, 287 (2000).
[46] T. Hu, H. Xiao, C. Visani, Z. Sefrioui, J. Santamaria, and C. C. Almasan, Phys. Rev. B **80**, 060506(R) (2009).